



## ARTICLE

# Analyzing the impact of quarantine and asymptomatic infection on the transmission dynamics of Covid-19

Chinelo Ujunwa Chikwelu,<sup>\*</sup><sup>1</sup> Julian Ibezimako Mbegbu,<sup>2</sup> and Friday Ewere<sup>2</sup>

<sup>1</sup>Department of Statistics, Faculty of Physical Sciences, Nnamdi Azikiwe University, P.O. Box 5025 Awka, Nigeria.

<sup>2</sup>Department of Statistics, Faculty of Physical Sciences, University of Benin, Benin City, Nigeria.

\*Corresponding author. Email: uc.anyadiegwu@unizik.edu.ng

(Received: August 11, 2025; Revised: December 19, 2025; Accepted: January 30, 2026; Published: June 05, 2026)

Section Editor: João Domingos Scalon

### Abstract

The global rapid spread of COVID-19, partially driven by asymptomatic undetected carriers, needs appropriate modeling to inform effective intervention strategies. This research develops and describes a deterministic compartmental model with six epidemiological classes: Susceptible (S), Exposed (E), Asymptomatic Infected ( $I_A$ ), Symptomatic Infected ( $I_S$ ), Quarantined (Q), and Recovered (R), all encompassing the  $SEI_A I_S QR$  framework. The model incorporates the progression of asymptomatic infections to symptomatic phases prior to progressing into quarantine, which captures realistic disease state progressions. By means of analytical methods, the basic reproduction number ( $R_0$ ) is derived from the next-generation matrix, and the local and global stability of the disease-free steady state are established under the  $R_0 < 1$  assumption. Sensitivity analysis reveals that transmission rates, progression rates, and quarantine policies drive  $R_0$ , and transmission through asymptomatic carriers is dominant. Euler's method-based numerical simulation shows that asymptomatic undetected carriers have a high contribution to persistent disease transmission, while effective quarantine and extensive recovery severely inhibit epidemic persistence. This paper stresses the critical necessity for robust public health measures involving mass testing, successful contact tracing, and isolation of asymptomatic patients in a bid to combat COVID-19.

**Keywords:** Deterministic model; COVID-19;  $SEI_A I_S QR$  model; Asymptomatic; Euler's method.

## 1. Introduction

Mathematical modeling transforms world problems into mathematical frameworks, enabling precise description and solutions for complex challenges which will be difficult to address using traditional strategies (Aakash *et al.*, 2024; Tang *et al.*, 2023; Ali *et al.*, 2023). "In the context of infectious diseases, these models are invaluable for understanding transmission dynamics and guiding control

measures” (Ndairou *et al.*, 2020). Classical models such as the SI, SIR, and SIRS frameworks have evolved into more sophisticated approaches tailored to address specific epidemiological challenges.

The 2019 novel coronavirus, officially named Severe Acute Respiratory Syndrome Coronavirus-2 (SARS-CoV-2), belongs to the coronavirus family, known for its crown-like appearance under an electronic microscope (WHO, 2020). Coronavirus can infect both humans and animals, causing a variety of diseases. The COVID-19 pandemic began in late 2019 in China and rapidly spread worldwide, posing a significant global health threat (Din *et al.*, 2020).

Transmission occurs primarily through respiratory droplets released during coughing, sneezing, or close interaction, typically within a distance of one meter (Chikwelu *et al.*, 2024). ‘These droplets can be inhaled or settled on surfaces, where the virus may survive for hours to days. Contact with contaminated surfaces, followed by touching the nose, mouth, or eyes can lead to infection. However, the infectious load on surface diminishes over time, potentially reducing the risk of transmission’ (Chikwelu *et al.*, 2024).

The incubation period for COVID-19 ranges from 5 to 14 days. Common side effects include fever, fatigue, and dry cough, while less frequent symptoms are diarrhea, headaches, sore throat, rashes, and loss of smell or taste. Severe symptoms such as chest pain, trouble in breathing, and loss of mobility or speech are more likely in severe cases. Older individuals and those with pre-existing conditions, including diabetes, cancer, cardiovascular infection, and constant respiratory illness, are at greater risk of severe complications (Aakash *et al.*, 2024).

To mitigate the spread of COVID-19, the following measures are recommended: maintain a minimum distance of one meter, avoid unnecessary travel and large gathering, wash hands frequently with soap and water or use hand sanitizer, refrain from smoking and excessive drinking to protect lungs health, and stay home if feeling unwell.

Various mathematical models have been developed to understand and predict the dynamics of the COVID-19 pandemic. Arino & Portet (2020) introduced an SLIAR disease model comprising eight differential equation compartments to study disease behaviour, turning points, and peak dynamics alongside sensitivity analysis. Bhattacharjee *et al.* (2021) used statistical method to predict the pandemic’s trend until June 2020, emphasizing the effectiveness of lockdowns and quarantine measures in reducing transmission. Li *et al.* (2020) investigated the role of mass flue inoculation and public health interventions in mitigating COVID-19 outbreaks. Tang *et al.* (2023) proposed a model highlighting the impact of fast testing and social separating on controlling disease spread. Benrhmach *et al.* (2020) highlighted the significant role of asymptomatic individuals in COVID-19 transmission and emphasized the significance of strict social distancing to prevent the healthcare system from being overwhelmed. Tomochi & Kono (2021) developed a model incorporating presymptomatic and asymptomatic populations, noting the challenges of isolating asymptomatic carriers. Danjuma *et al.* (2024) presented a deterministic model assessing the effectiveness of social distancing, facemask use, and hospitalization. Their findings suggested that a combined approach significantly reduces the infection burden. Zeb *et al.* (2020) focused on the isolation of infected individuals, showing that reducing effective contact with infected persons is crucial for controlling the pandemic.

While many existing models assume direct recovery for asymptomatic individuals, this study introduces a framework where asymptomatic individuals transit to symptomatic status before moving into quarantine. The primary objective is to evaluate the effectiveness of quarantine measures and the impact of asymptomatic individuals in the transmission dynamics of COVID-19 using the  $SEI_A I_S QR$  deterministic model.

## 2. Model Formulation

The total population at any given time, represented as  $N(t)$ , is divided into six categories: the susceptible group  $S(t)$ , the exposed group  $E(t)$  the asymptomatic infected group  $I_A(t)$ , the symptomatic infected group  $I_S(t)$ , the quarantine group  $Q(t)$ , and the recovered group  $R(t)$ .

### Model Assumptions

- The population is dynamic and homogenously mixed, meaning every individual has an equal chance of being infected upon contact with an infectious person.
- Recruitment into the population occurs at a constant rate through immigration.
- Susceptible individuals are presumed to become infected through interaction with infected individuals.
- Asymptomatic individuals transit to symptomatic category
- Symptomatic individuals are assumed to enter the quarantine group upon exhibiting symptoms.
- Following treatment, quarantine individuals move to the recovered group.
- Disease-induced mortality occurs in infectious and quarantine class, while Natural death occurs uniformly across all compartments.

Based on this classification, a foundational nonlinear mathematical model is developed as follows.

$$\begin{aligned}
 \frac{dS}{dt} &= \Pi - \rho_1 \beta_A I_A S - \rho_2 \beta_S I_S S - \mu S + \rho R \\
 \frac{dE}{dt} &= \rho_1 \beta_A I_A S + \rho_2 \beta_S I_S S - (\alpha + \mu) E \\
 \frac{dI_A}{dt} &= \alpha(1 - \delta) E - (\gamma + \mu_x + \mu) I_A \\
 \frac{dI_S}{dt} &= \delta \alpha E + \gamma I_A - (\omega + \mu_x + \mu) I_S \\
 \frac{dQ}{dt} &= \omega I_S - (\theta + \mu_x + \mu) Q \\
 \frac{dR}{dt} &= \theta Q - \mu R - \rho R
 \end{aligned} \tag{1}$$

The parameter for model (1) are described in Table (1) and Figure (1) illustrate the schematic diagram of our model.

**Table 1.** Description of parameters

Parameter	Description
$\Pi$	Recruitment rate
$\beta_A$	Transmission probability from asymptomatic infectious to susceptible
$\beta_S$	Transmission probability from symptomatic infectious to susceptible
$\rho_1$	Contact rate of symptomatic individuals
$\rho_2$	Contact rate of asymptomatic individuals
$\rho$	Rate of immunity loss
$\delta$	is a fraction that determine the population of those who become symptomatic.
$\alpha$	Total rate of progression from exposed to infectious state
$\mu$	Natural death rate
$\omega$	Quarantine rate from symptomatic infectious class ( $I_S$ )
$\gamma$	Progression rate from asymptomatic ( $I_A$ ) to symptomatic class
$\mu_x$	Death due to disease
$\theta$	Recovery rate from quarantined class to recovered class

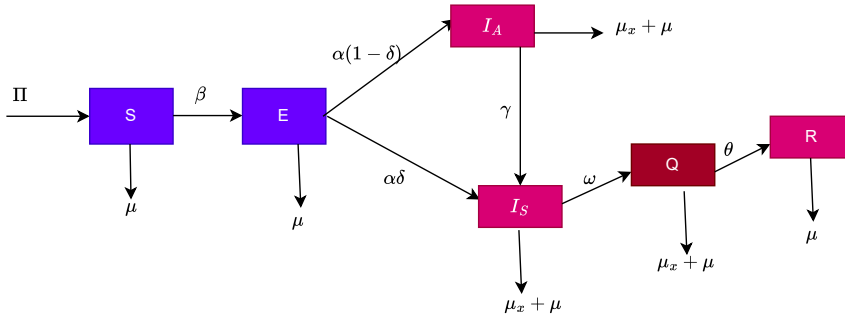


Figure 1. The schematic diagram of the  $SEI_A I_S QR$  Model.

### 3. Local Asymptotic Stability (LAS) of the Disease-free Equilibrium (DFE)

The equilibrium of our model is found by equating the right hand side of the compartmental model (1) to zero.

$$(S^0, E^0, I_A^0, I_S^0, Q^0, R^0) = \left( \frac{\Pi}{\mu}, 0, 0, 0, 0, 0 \right) \quad (2)$$

Linear stability of  $\epsilon_0$  is determined by providing next-generation method of operation in the model system 1.

The specific notation represented by Van den Driessche & Watmough (2002) will be given by the matrix  $F$  (from fresh infections) and  $V$  (movement of people between classes), respectively are given by.

$$F = \begin{pmatrix} 0 & \rho_1 \beta_A \frac{\Pi}{\mu} & \rho_2 \beta_S \frac{\Pi}{\mu} \\ 0 & 0 & 0 \\ 0 & 0 & 0 \end{pmatrix}, \quad V = \begin{pmatrix} \alpha + \mu & 0 & 0 \\ -\alpha(1-\delta) & \gamma + \mu + \mu_x & 0 \\ -\delta\alpha & -\gamma & \omega + \mu + \mu_x \end{pmatrix}$$

Hence,  $R_0 = \kappa(FV^{-1})$  where  $\kappa$  is the spectral radius (principal eigenvalue in magnitude) of the next generation matrix given by:

$$R_0 = \left[ \frac{\Pi \rho_1 \beta_A \alpha (1-\delta)}{\mu((\alpha + \mu)(\gamma + \mu + \mu_x))} + \frac{\Pi \rho_2 \beta_S \alpha [\delta(\gamma + \mu + \mu_x) + (1-\delta)\gamma]}{\mu(\alpha + \mu)(\gamma + \mu + \mu_x)(\omega + \mu + \mu_x)} \right] \quad (3)$$

Thus, the ensuing outcome is a corollary of the conclusion of Theorem 2 in Van den Driessche & Watmough (2002)

**Theorem 1:** The DFE  $\epsilon_0$  is locally asymptotically stable if and only if  $R_0 < 1$  and unstable if and only if  $R_0 > 1$ . The key quantity,  $R_0$ , is the disease's basic reproduction number. It measures the average number of secondary cases of COVID-19 caused by an average infected individual within a fully exposed population or at the DFE.

**Proof of Local Stability:** To support this result, we examine the Jacobian matrix of the system 1 evaluated at the DFE  $\epsilon_0$ . The linearized stability of the system is determined by the eigenvalues of

the following matrix,

$$J(\epsilon_0) = \begin{pmatrix} -\mu & 0 & -\rho_1 \beta_A S^0 & \rho_2 \beta_S S^0 & 0 & \rho \\ 0 & -(\alpha + \mu) & \rho_1 \beta_A S^0 & \rho_2 \beta_S S^0 & 0 & 0 \\ 0 & \alpha(1 - \delta) & -(\gamma + \mu_x + \mu) & 0 & 0 & 0 \\ 0 & \delta \alpha & \gamma & -(\omega + \mu_x + \mu) & 0 & 0 \\ 0 & 0 & 0 & \omega & -(\theta + \mu_x + \mu) & 0 \\ 0 & 0 & 0 & 0 & \theta & -(\mu + \rho) \end{pmatrix}$$

The characteristic equation of  $J(\epsilon_0)$  reveals that all eigenvalues have negative real parts if and only if  $R_0 < 1$ . This confirms that the system is locally stable, meaning the disease will die out following a small perturbation near the equilibrium point.

The epidemiological connotation of Theorem 1 implies that whenever  $R_0$  is less than one, COVID-19 can be eradicated from the population if the initial sizes of the classes of the model system are in the basin of attraction of the infection-free equilibrium  $\epsilon_0$ . Accordingly, a low number of COVID-19-infected human beings in the population will not result in humongous cases of COVID-19, with the net effect being the extinction of the disease in the long term.

## 4. Endemic Equilibrium Point (EEP)

For model (1), we got the endemic equilibrium as

$$P_1 = (S^*, E^*, I_A^*, I_S^*, Q^*, R^*) \quad (4)$$

where

$$\begin{aligned} S^* &= \frac{\Pi + \rho R^* - a_1 E^*}{\mu} \\ E^* &= \frac{\Pi}{\delta + \alpha + \mu} \left(1 - \frac{1}{R_0}\right) \\ I_A^* &= \frac{\alpha(1 - \delta)\Pi}{(\alpha + \mu)(\gamma + \mu + \mu_x)} \left(1 - \frac{1}{R_0}\right) \\ I_S^* &= \frac{\Pi}{(\alpha + \mu)(\omega + \mu + \mu_x)} \left[\alpha\delta + \frac{\gamma\alpha(1 - \delta)}{\gamma + \mu + \mu_x}\right] \left(1 - \frac{1}{R_0}\right) \\ Q^* &= \frac{\omega\Pi}{(\theta + \mu + \mu_x)(\omega + \mu + \mu_x)(\alpha + \mu)} \left[\alpha\delta + \frac{\gamma\alpha(1 - \delta)}{\gamma + \mu + \mu_x}\right] \left(1 - \frac{1}{R_0}\right) \\ R^* &= \frac{\theta\omega\Pi}{\mu(\theta + \mu + \mu_x)(\omega + \mu + \mu_x)(\alpha + \mu)} \left[\alpha\delta + \frac{\gamma\alpha(1 - \delta)}{\gamma + \mu + \mu_x}\right] \left(1 - \frac{1}{R_0}\right) \end{aligned} \quad (5)$$

## 5. Global Asymptotic Stability (GAS) of the Disease Free Equilibrium

To ensure that the eradication of COVID-19 is independent of the initial population size in the model, it is crucial to demonstrate that the Disease Free Equilibrium (DFE) of Eq. (1) is globally asymptotically stable. To establish this, we adopt the approach by Chavez *et al.* (2002).

**Lemma 1** Chavez *et al.* (2002): Consider the system of Eq. (1), which can be expressed as follows:

Consider a system of the form

$$\begin{aligned}\frac{dU_1}{dt} &= V(U_1, U_2), \\ \frac{dU_2}{dt} &= Z(U_1, U_2), \quad \text{with } Z(U_1, 0) = 0,\end{aligned}$$

Here,  $U_1 \in \mathbb{R}^m$  represents the components of the uninfected population classes which includes susceptible class ( $S$ ) and recovered class ( $R$ ), while  $U_2 \in \mathbb{R}^n$  represents the components of the infected compartments. These include the exposed class ( $E$ ), asymptomatic infected ( $I_A$ ), symptomatic infected ( $I_S$ ), and the quarantine class ( $Q$ ). Additionally, two assumptions are required:

where  $U_1 \in \mathbb{R}^m$  represents uninfected compartments, and  $U_2 \in \mathbb{R}^n$  represents infected compartments. Suppose the following two conditions hold:

- 1 The subsystem  $\frac{dU_1}{dt} = V(U_1, 0)$  has a globally asymptotically stable equilibrium  $U_1^*$ .
- 2  $Z(U_1, U_2) = WU_2 - \hat{Z}(U_1, U_2)$ ,

where  $W = D_{U_2}Z(U_1^*, 0)$  is a Metzler matrix (i.e., all off-diagonal entries are nonnegative), and  $\hat{Z}(U_1, U_2) \geq 0$  for all  $(U_1, U_2) \in \Omega$ .

**Lemma 2:** The fixed point  $U_0 = (U_1^*, 0)$  is globally asymptotically stable for the model described by system (1), provided that  $R_0 < 1$  and that the assumptions 1, and 2 hold.

**Theorem 2:** The disease-free equilibrium  $P_0 = \left(\frac{\pi}{\mu}, 0, 0, 0, 0, 0\right)$  of system (1) is globally asymptotically stable if  $\mathcal{R}_0 < 1$ .

**Proof:** To demonstrate this, we adopt the notation introduced in lemma 1 and verify that the assumption 1 and 2 hold for our model

$$U_1 = \begin{pmatrix} S \\ R \end{pmatrix}, \quad U_2 = \begin{pmatrix} E \\ I_A \\ I_S \\ Q \end{pmatrix}, \quad U_1^* = \begin{pmatrix} \frac{\pi}{\mu} \\ 0 \end{pmatrix}.$$

Uninfected subsystem is

$$\frac{d}{dt} \begin{pmatrix} S \\ R \end{pmatrix} = \begin{pmatrix} \pi - \rho_1 \beta_A I_A S - \rho_2 \beta_S I_S S - \mu S + \rho R \\ \theta Q - (\mu + \rho) R \end{pmatrix} \quad (6)$$

At the DFE ( $I_A = I_S = Q = 0$ ), this reduces to:

$$\frac{d}{dt} \begin{pmatrix} S \\ R \end{pmatrix} = \begin{pmatrix} \pi - \mu S \\ -\mu R \end{pmatrix} \quad (7)$$

The solutions are:

$$R(t) = R(0)e^{-\mu t}, \quad S(t) = \left(S(0) - \frac{\pi}{\mu}\right) e^{-\mu t} + \frac{\pi}{\mu},$$

which implies:

$$S(t) \rightarrow \frac{\pi}{\mu}, \quad R(t) \rightarrow 0 \quad \text{as } t \rightarrow \infty.$$

Thus,  $U_1^* = \left(\frac{\pi}{\mu}, 0\right)$  is globally asymptotically stable. Hence, condition 1 is satisfied.

Infected subsystem and Metzler matrix.

We compute the Jacobian of  $Z$  with respect to  $U_2$  at the DFE:

$$W = \frac{\partial Z}{\partial U_2} \Big|_{U_1=U_1^*, U_2=0} = \begin{pmatrix} -(\alpha + \mu) & \rho_1 \beta_A S^0 & \rho_2 \beta_S S^0 & 0 \\ \alpha(1 - \delta) & -(\gamma + \mu_x + \mu) & 0 & 0 \\ \alpha\delta & \gamma & -(\omega + \mu_x + \mu) & 0 \\ 0 & 0 & \omega & -(\theta + \mu_x + \mu) \end{pmatrix} \quad (8)$$

with  $S^0 = \frac{\Pi}{\mu}$ .

Since all off-diagonal entries are nonnegative, the matrix is Metzler, .

We now define:

$$\hat{Z}(U_1, U_2) = WU_2 - Z(U_1, U_2)$$

$$Z(U_1, U_2) = \begin{bmatrix} \rho_1 \beta_A I_A \frac{\Pi}{\mu} + \rho_2 \beta_S I_S \frac{\Pi}{\mu} - (\alpha + \mu)E \\ \alpha(1 - \delta)E - (\gamma + \mu_x + \mu)I_A \\ \alpha\delta E + \gamma I_A - (\omega + \mu_x + \mu)I_S \\ \omega I_S - (\theta + \mu_x + \mu)Q \end{bmatrix}$$

Explicit computation gives:

$$\hat{Z}(U_1, U_2) = \begin{pmatrix} \rho_1 \beta_A I_A (S^0 - S) + \rho_2 \beta_S I_S (S^0 - S) \\ 0 \\ 0 \\ 0 \end{pmatrix} \quad (9)$$

which is clearly nonnegative for  $S \leq S^0$ . Hence,  $\hat{Z}(U_1, U_2) \geq 0$  in the region  $\Omega$ .

Thus, assumption 2 is satisfied.

**Conclusion:** By Lemma 1, the DFE is globally asymptotically stable whenever  $\mathcal{R}_0 < 1$ .

## 6. Sensitivity Analysis

We performed a sensitivity analysis of the  $R_0$  with respect to parameters of the model (1), which includes the population recruitment rate  $\Pi$ , transmission rates for symptomatic and asymptomatic infections ( $\beta_A, \beta_S$ ), contact rates for symptomatic and asymptomatic infections ( $\rho_1, \rho_2$ ), the fraction that determine the population of those who become symptomatic ( $\delta$ ), the total rate of progression from exposed to infectious state ( $\alpha$ ), the natural death rate ( $\mu$ ), the quarantine rate ( $\omega$ ), the proportion of individuals transitioning from the asymptomatic to symptomatic class ( $\gamma$ ), the recovery rate ( $\theta$ ), the rate of immunity loss ( $\rho$ ) and the COVID-19 induced death rate ( $\mu_x$ ). To compute this, we employed the normalized forward sensitivity index, using the formula provided by Chitnis *et al.* (2008).

$$A_{\Phi}^{(R_0)} = \frac{\partial R_0}{\partial \Phi} \cdot \frac{\Phi}{R_0}$$

The sensitivity index values for parameters specified in Table (3) are presented in Table (2) and pictorially shown in Figure (2). The sensitivity index value of +1 or -1 means that a relative change or reduction in the parameter  $\Phi$  will lead to an equivalent percentage change in the basic reproduction number  $R_0$ . Sensitive parameters must be estimated with much caution since slight variations have the ability to affect the model a great deal. Parameters that possess low sensitivity indices have hardly any effect on the outcome and can be estimated more flexibly. According to Table (2), the largest affecting parameters of  $R_0$  in the COVID-19 model (1) are  $\beta_S, \rho_2$ , and  $\alpha$ . Interestingly, both the increase of  $\beta_S$  and  $\rho_2$  add up 58.55% to  $R_0$ , and an increase of  $\alpha$  adds 99.65% to  $R_0$ . In addition, an increase of  $\Pi$  increases  $R_0$  by 100%.

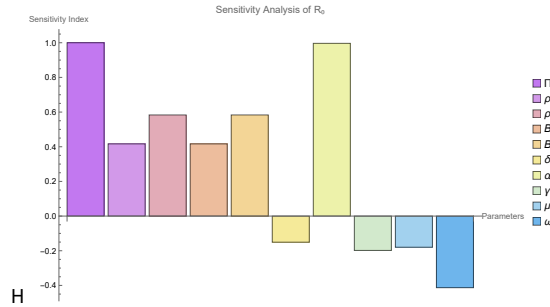


**Figure 2.** Sensitivity Analysis of  $R_0$ .

**Table 2.** Sensitivity of  $R_0$  evaluated for the parameter values

Parameter	Sensitivity index
$\Pi$	1.00
$\rho_1$	0.416
$\rho_2$	0.584
$\beta_A$	0.416
$\beta_S$	0.584
$\delta$	-0.151
$\alpha$	0.997
$\gamma$	-0.198
$\mu_x$	-0.180
$\omega$	-0.413

## 7. Numerical Simulation and Discussion

In this section, we discuss the numerical simulation of model (1). The mathematical procedure used is based on Euler's method implemented in R. Note that the initial conditions used for the simulation and the parameter values are given in Table (3)

**Table 3.** Sensitivity of  $R_0$  evaluated for the parameter values

Parameter	Values	References
$S(0)$	500	(Abioye <i>et al.</i> , 2021)
$E(0)$	2003	(Abioye <i>et al.</i> , 2021)
$I_S(0)$	416	(Abioye <i>et al.</i> , 2021)
$I_A(0)$	1000	(Abioye <i>et al.</i> , 2021)
$Q(0)$	404	(Abioye <i>et al.</i> , 2021)
$R(0)$	115	(Abioye <i>et al.</i> , 2021)
$\Pi$	$750 \text{ day}^{-1}$	(Krishna & Prakash, 2020)
$\beta_A$	0.000062	Calculated
$\beta_S$	0.0000124	(Abioye <i>et al.</i> , 2021)
$\alpha$	$0.000011618 \text{ day}^{-1}$	(Abioye <i>et al.</i> , 2021)
$\delta$	0.3 dimensionless	(Iboi <i>et al.</i> , 2020)
$\omega$	0.015	Assumed
$\gamma$	0.015	(Chikwelu <i>et al.</i> , 2024)
$\mu_x$	0.00286	(Abioye <i>et al.</i> , 2021)
$\theta$	0.0766169	(Abioye <i>et al.</i> , 2021)
$\rho_S$	0.589	(Iboi <i>et al.</i> , 2020)
$\rho_A$	0.331	(Iboi <i>et al.</i> , 2020)
$\mu$	0.003324588	(Abioye <i>et al.</i> , 2021)
$\rho$	0.000001	Assumed

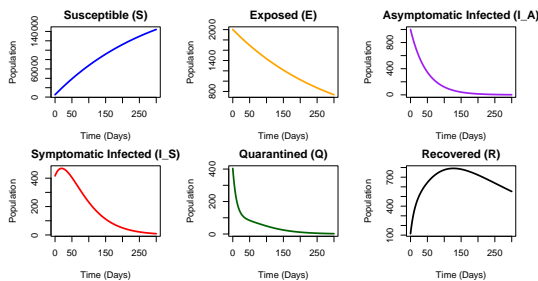


**Figure 3.** Transmission dynamics of the Disease Free Equilibrium for  $SELAISQR$  model.

Figure (3) illustrates the time course of six compartments of the COVID-19 spread model: Susceptible (S), Exposed (E), Asymptomatic Infected ( $I_A$ ), Symptomatic Infected ( $I_S$ ), Quarantined (Q), and Recovered (R), over a simulation duration of 250 days. Together, these graphs illustrate the dynamics of epidemic spread and the effect of different control measures in the population under the assumed parameter values.

**Susceptible (S):** Susceptible population size declines steadily over time, suggesting continued exposure to infectious classes. The drop shows active transmission as individuals get infected and progress into the exposed compartment. The absence of a plateau suggests transmission pressure is sustained in the early and middle stages of the epidemic.

**Exposed (E):** The infected compartment initially increases, peaks, then declines. This curve characterized by an initial increase in the number of new infections followed by a slow decline as the number of susceptible individuals reduces and interventions, such as isolation and recovery, begin to take effect.

Asymptomatic Infected ( $I_A$ ): A rapid initial increase in the asymptomatic infected class is followed by a decline. The relatively high peak in this compartment indicates that a significant proportion of infected individuals are asymptomatic, yet infectious. Such asymptomatic transmission presents a tremendous challenge to containment, as these individuals typically go undetected and unquarantined.

Symptomatic Infected ( $I_S$ ): The symptomatic infected category features a lower peak and more delayed development than  $I_A$ . This suggests that symptomatic cases are more successfully managed through quarantine, so their transmission role is shortened. It also shows that not all of the exposed cases develop to symptomatic illness.

Quarantined (Q): The quarantined population grows modestly, then shrinks, which is a reflection of moderate levels of quarantine enforcement. The relatively small size of this compartment suggests that only a proportion of infectious individuals are being quarantined and detected, those who are symptomatic.

Recovered (R): The recovered subjects monotonically rise and form the largest compartment in the end. The trend suggests that the majority of infections are resolved by recovery in the long term, draining active cases and building population-level immunity. The dominance of this group in the latter half of the simulation suggests successful long-term management of the outbreak.

Implications of Asymptomatic Transmission on Disease Control A key observation in the simulation is the significant role played by asymptomatic carriers ( $I_A$ ) in the persistence of transmission. The steep and early rise in  $I_A$ , outstripping that of the symptomatic class  $I_S$  suggests that the majority of infections are asymptomatic. Such covert transmission presents a formidable obstacle to control, as these individuals are less likely to be detected or quarantined.

Due to their continued mixing with the general population, asymptomatics contribute disproportionately to continued transmission. Their impact extends the lag in the decay of the susceptible pool and the duration of the epidemic. Symptomatic cases, in contrast, become increasingly likely to be identified and removed from the chain of transmission through quarantine.

Furthermore, the fact that the quarantined population is small corroborates the result that a high number of infectious individuals are beyond the reach of public health containment strategies. This indicates one of the primary limitations: even if there are efficient recovery and quarantine mechanisms in place, the inability to identify and isolate asymptomatic cases significantly compromises the overall effectiveness of disease control.

With these findings, more severe surveillance strategies, such as large-scale testing, rigorous contact tracing, and targeted or presumptive quarantine, must be taken to effectively address the hidden spread of asymptomatic transmission and achieve robust epidemic control.

Figures (4 - 9) provide surface plots of the variation of the basic reproduction number  $R_0$  with respect to significant epidemiological parameters. Graphical analysis provides information about the influence of each of the control measures and biological processes on potential disease spread.

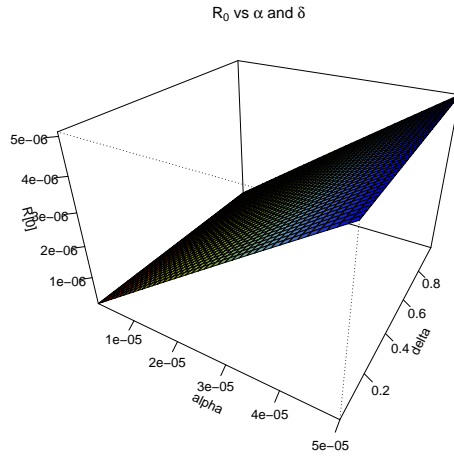


Figure 4. Surface plot of  $R_0$  with respect to  $\alpha$  and  $\delta$ .

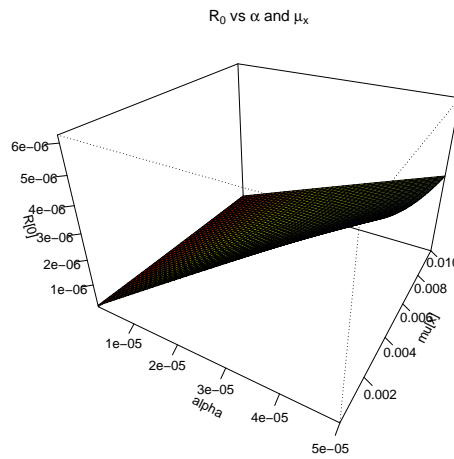


Figure 5. Surface plot of  $R_0$  with respect to  $\alpha$  and  $\mu_x$ .

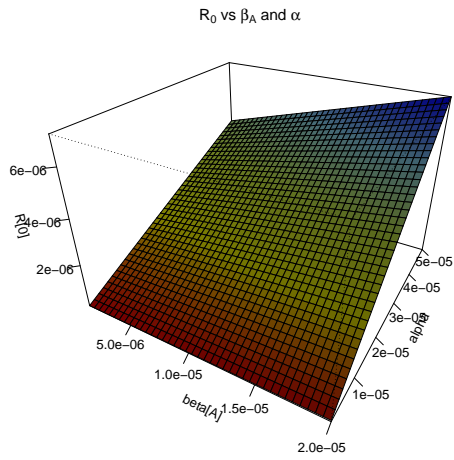


Figure 6. Surface plot of  $R_0$  with respect to  $\beta_A$  and  $\alpha$ .

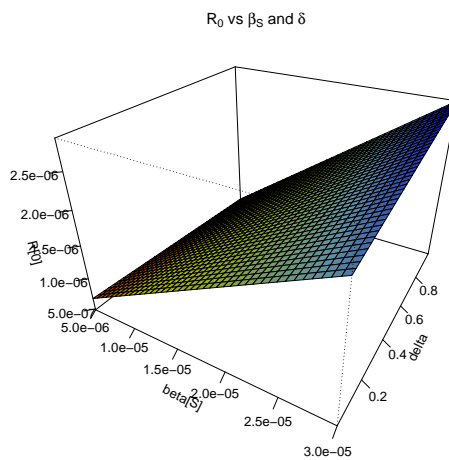


Figure 7. Surface plot of  $R_0$  with respect to  $\beta_S$  and  $\delta$ .

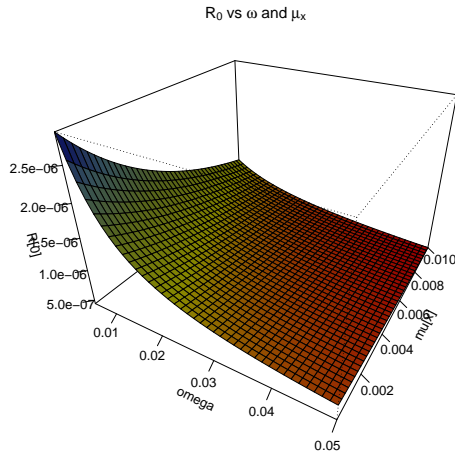


Figure 8. Surface plot of  $R_0$  with respect to  $\omega$  and  $\mu_x$ .

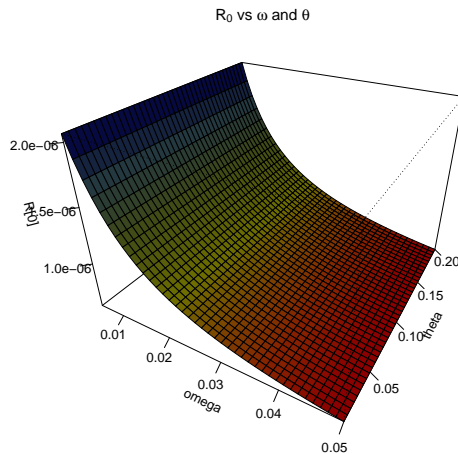


Figure 9. Surface plot of  $R_0$  with respect to  $\omega$  and  $\theta$ .

Figure (4) here presents how  $R_0$  varies with  $\alpha$ , which is the fraction of the population who become symptomatic, and  $\delta$ , which is the progression rate from the exposed to the infectious class. The surface plot indicates a decreasing trend in  $R_0$  when either  $\alpha$  or  $\delta$  increases. This indicates that greater detection (as represented by larger  $\alpha$ ) or faster progression through the exposed phase (represented by higher  $\delta$ ) are both effective in reducing the overall potential for spread of disease.

Figure (5) considers the interactive effect of  $\alpha$  and the disease-caused mortality rate ( $\mu_x$ ). With both parameters increasing, there is a consistent decrease in  $R_0$ . This suggests that improved case detection and the management of fatal cases, through quarantine or intensive care, can reduce the infectious period or the number of infectious carriers, thereby reducing  $R_0$ .

Figure (6) is concerned with the relationship between the asymptomatic transmission rate ( $\beta_A$ )

and the progression rate ( $\alpha$ ). The results indicate that  $R_0$  rises with increased levels of  $\beta_A$ , emphasizing the contribution of asymptomatic cases to maintaining transmission. On the other hand, rising  $\alpha$  causes  $R_0$  to decrease, showing that earlier diagnosis and quicker passage through infectious stages can reduce the impact of asymptomatic transmission. Additionally, even under high asymptomatic transmission circumstances, a sufficiently large  $\alpha$  can counteract the probability of mass infection.

Figure (7) illustrates the impact of the symptomatic transmission rate ( $\beta_S$ ) and progression rate ( $\delta$ ). As would be expected, bigger  $\beta_S$  values are associated with bigger  $R_0$ , in terms of more transmission from symptomatic cases. Making  $\delta$  bigger reduces  $R_0$  significantly, showing the benefit of restricting how long people remain in the exposed or infectious classes.

Figure (8) shows the impact of quarantine rate ( $\omega$ ) and mortality rate ( $\mu_x$ ) on  $R_0$ . The graph has a negative slope of  $R_0$  as the parameter is increased. The negative slope shows that rapid quarantine of infected people and early disposal of critical cases (death or recovery) contribute to reducing the disease spread. Increased  $\omega$  values represent more effective isolation strategies, and rises in  $\mu_x$  represent removals from the transmission pool, either through death or clinical intervention.

Figure (9) explores the combined effect of the quarantine rate for symptomatic individuals ( $\omega$ ) and recovery rate ( $\theta$ ). The graph clearly demonstrates that  $R_0$  consistently reduces with the increase of any of these parameters. Extended quarantine periods reduce the infectious duration of symptomatic carriers in the population, and heightened recovery rates reduce the infectious duration altogether. Both results together severely limit transmission. Of significance, across all value ranges explored,  $R_0$  is substantially less than unity, indicating that the disease won't take hold under such circumstances. This observation further supports that with effective control measures, particularly among the asymptomatic and symptomatic ones, the likelihood of a sustained outbreak can be minimized.

In general, these results indicate that timely interventions like early diagnosis, effective quarantine, rapid recovery, and reduced contact rates are critical in controlling the transmission of the infection. The findings necessitate public health interventions that improve surveillance, isolation, and treatment to maintain  $R_0 < 1$  and ensure effective control of the disease.

### Public Health Policy Implication:

In the  $SEI_A I_S QR$  model, the analysis shows that the critical paths in the model are essential for the control of the COVID-19 pandemic. From the results, it is shown that using the quarantine method on symptomatic cases alone is inadequate since the asymptomatic cases,  $I_A$ , play a major role in the disease transmission process among the whole population. Therefore, the following interventions are proposed based on the model analysis results:

**Increased Surveillance of Asymptomatic Carriers:** Because of the substantial contribution of  $I_A$  to  $R_0$ , epidemic control policies must change from Passive Testing (testing individuals who are symptomatic) to Active Surveillance. This would involve mass testing and surveillance in densely populated areas to identify "hidden" carriers before they have the opportunity of infecting the Susceptible individuals.

**Maximizing the Efficiency of Quarantine:** Sensitivity analysis indicates that raising the rate of quarantined individuals ( $\omega$ ) who are symptomatic reduces the value of  $R_0$ . The model indicates that the critical focus must be to minimize the time period within which a symptomatic individual is removed from the chain of communication.

**Targeted Contact Tracing:** The model emphasizes that even under conditions of efficient recovery rates, failure to identify asymptomatic cases undermines control. Rigorous contact tracing is required to "unmask"  $I_A$  individuals who are either in latent or asymptomatic phases, thereby effectively transferring them into the quarantine (Q) compartment much earlier.

## 8. Conclusion

This work presents a deterministic  $SEI_AISQR$  model to explore COVID-19 transmission dynamics with the role of quarantine and asymptomatic infections.

Analytical results prove that whenever the basic reproduction number  $R_0$  is less than one, the disease-free equilibrium is locally and globally asymptotically stable, which indicates the potential for eradication by effective control efforts.

Sensitivity analysis identifies symptomatic and asymptomatic carriers' transmission probabilities, contact rates, and the rate of progression from exposure to infectivity as significant parameters upon which  $R_0$  relies. Simulation result illustrates that asymptomatic individuals, who are likely to evade detection and quarantine, contribute considerably to sustained spread. This covert spread foils control and slows down epidemic closure even when symptomatic cases are efficiently controlled.

The outcomes point to the importance of expanding surveillance to asymptomatic carriers through mass testing and contact tracing. Public health measures should maximize rapid detection, selective quarantine, and increased recovery rates to limit transmission and push  $R_0$  below the threshold. The model overall promotes building sound methods that address both manifest and hidden infection pathways to facilitate sustainable epidemic control.

## Acknowledgments

The authors are deeply indebted to the editors and learned reviewers for their valuable comments improving the original manuscript's contents and presentation.

## Conflicts of Interest

The authors declare no conflict of interest.

## Author Contributions

**Conceptualization:** CHIKWELU, C.U.; MBEGBU, I. J.; EWERE, F. **Data curation:** CHIKWELU, C.U. **Formal analysis:** CHIKWELU, C.U. **Investigation:** CHIKWELU, C.U.; MBEGBU, I. J.; EWERE, F. **Methodology:** CHIKWELU, C.U.; MBEGBU, I. J.; EWERE, F. **Project administration:** ; MBEGBU, I. J.; EWERE, F. **Software:** CHIKWELU, C.U. **Resources:** CHIKWELU, C.U.; MBEGBU, I. J.; EWERE, F. **Supervision:** ; MBEGBU, I. J.; EWERE, F. **Validation:** CHIKWELU, C.U.; MBEGBU, I. J.; EWERE, F. **Visualization:** CHIKWELU, C.U. **Writing - original draft:** CHIKWELU, C.U.; MBEGBU, I. J.; EWERE, F. **Writing - review and editing:** CHIKWELU, C.U.; MBEGBU, I. J.; EWERE, F.

## References

1. Aakash, M, Gunasundari, C, Athithan, S, Sharmila, N., Kumar, G. S. & Guefaifa, R. Mathematical modeling of COVID-19 with the effects of quarantine and detection. *Partial Differential Equations in Applied Mathematics* **9**, 100609. doi:10.1016/j.padiff.2023.100609 (2024).
2. Abioye, A. I., Peter, O. J., Ogunseye, H. A., Oguntolu, F. A., Oshinubi, K., Ibrahim, A. A. & Khan, I. Mathematical model of COVID-19 in Nigeria with optimal control. *Results in Physics* **28**, 104598. doi:10.1016/j.rinp.2021.104598 (2021).
3. Ali, A., Althobaiti, S., Althobaiti, A., Khan, K. & Jan, R. Chaotic dynamics in a non-linear tumor-immune model with Caputo–Fabrizio fractional operator. *The European Physical Journal Special Topics* **232**, 2513–2529. doi:10.1140/epjs/s11734-023-00929-y (2023).
4. Arino, J. & Portet, S. A simple model for COVID-19. *Infectious Disease Modelling* **5**, 309–315. doi:10.1016/j.idm.2020.04.002 (2020).

5. Benrhmach, G., Namir, K. & Bouyaghroumni, J. Modelling and simulating the novel coronavirus with implications of asymptomatic carriers. *International Journal of Differential Equations* **2020**, 5487147. doi:10.1016/j.cegh.2020.06.004 (2020).
6. Bhattacharjee, A., Kumar, M. & Patel, K. K. When COVID-19 will decline in India? Prediction by combination of recovery and case load rate. *Clinical Epidemiology and Global Health* **9**, 17–20. doi:10.1016/j.cegh.2020.06.004 (2021).
7. Chavez, C. C., Feng, Z & Huang, W. On the computation of  $R_0$  and its role on global stability. *Mathematical approaches for emerging and re-emerging infection diseases: An introduction* **125**, 31–65 (2002).
8. Chikwelu, C., Ewere, F & Mbegbu, J. Stochastic Modeling of COVID-19: A SEIAISQR-type model. *Benin Journal of Statistics* **7**, 29–43 (2024).
9. Chitnis, N., Hyman, J. M. & Cushing, J. M. Determining important parameters in the spread of malaria through the sensitivity analysis of a mathematical model. *Bulletin of mathematical biology* **70**, 1272–1296. doi:10.1007/s11538-008-9299-0 (2008).
10. Danjuma, R. U., Okolo, P. N. & Dauda, M. K. Mathematical modelling of COVID-19 transmission dynamics in Kaduna State, Nigeria. *Science World Journal* **19**, 1128–1142. doi:10.4314/swj.v19i4.31 (2024).
11. Din, A., Khan, A. & Baleanu, D. Stationary distribution and extinction of stochastic coronavirus (COVID-19) epidemic model. *Chaos, Solitons & Fractals* **139**, 110036. doi:10.1016/j.chaos.2020.110036 (2020).
12. Iboi, E., Sharomi, O. O., Ngonghala, C. & Gumel, A. B. Mathematical modeling and analysis of COVID-19 pandemic in Nigeria. *MedRxiv*, 2020–05. doi:10.1101/2020.05.22.20110387 (2020).
13. Krishna, M. V. & Prakash, J. Mathematical modelling on phase based transmissibility of Coronavirus. *Infectious Disease Modelling* **5**, 375–385. doi:10.1016/j.idm.2020.06.005 (2020).
14. Li, Q., Tang, B., Bragazzi, N. L., Xiao, Y. & Wu, J. Modeling the impact of mass influenza vaccination and public health interventions on COVID-19 epidemics with limited detection capability. *Mathematical biosciences* **325**, 108378. doi:10.1016/j.mbs.2020.108378 (2020).
15. Ndairou, F., Area, I., Nieto, J. J. & Torres, D. F. Mathematical modeling of COVID-19 transmission dynamics with a case study of Wuhan. *Chaos, Solitons & Fractals* **135**, 109846. doi:10.1016/j.chaos.2020.109846 (2020).
16. Tang, T.-Q., Jan, R., Khurshaid, A., Shah, Z., Vrinceanu, N. & Racheriu, M. Analysis of the dynamics of a vector-borne infection with the effect of imperfect vaccination from a fractional perspective. *Scientific reports* **13**, 14398. doi:10.1038/s41598-023-41440-7 (2023).
17. Tomochi, M. & Kono, M. A mathematical model for COVID-19 pandemic—SIIR model: Effects of asymptomatic individuals. *Journal of general and family medicine* **22**, 5–14. doi:10.1002/jgf2.382 (2021).
18. Van den Driessche, P. & Watmough, J. Reproduction numbers and sub-threshold endemic equilibria for compartmental models of disease transmission. *Mathematical biosciences* **180**, 29–48. doi:10.1016/S0025-5564(02)00108-6 (2002).
19. Zeb, A., Alzahrani, E., Erturk, V. S. & Zaman, G. Mathematical model for coronavirus disease 2019 (COVID-19) containing isolation class. *BioMed research international* **2020**, 3452402. doi:10.1155/2020/3452402 (2020).